

LEVEL

12

AD A099478



DTIC
SELECTED
MAY 29 1981

C

DISTRIBUTION STATEMENT A
Approved for public release;
Distribution Unlimited

SCIENCE APPLICATIONS, INC.

TIC FILE COPY

Best Available Copy

0 1 5 3 0 0 0 1

12

6 BOTTOM LOSS UPGRADE.
 9 Final Report.
 1 Apr - 1 Jun 81,
 14 SAI-82-488-WA

11 May 81

12 29

10 E. / Michelson
 L. / Dozier
 A. / Stokes
 R. / Green

DTIC ELECTE
 MAY 29 1981
 S D C

15 N00014-79-C-0370

DISTRIBUTION STATEMENT A
 Approved for public release;
 Distribution Unlimited



ATLANTA • ANN ARBOR • BOSTON • CHICAGO • CLEVELAND • DENVER • HUNTSVILLE • LA JOLLA
 LITTLE ROCK • LOS ANGELES • SAN FRANCISCO • SANTA BARBARA • TUCSON • WASHINGTON

408404

28 May 1981

Scientific Officer
Ocean Programs Office
Naval Ocean Research and
Development Activity
(NORDA Code 500)
NSTL Station, MS 39529



ATTN: Mr. E. D. Chaika:

Dear Sir:

The Ocean Acoustics Division of Science Applications, Inc. is pleased to deliver the final report for ONR Contract N00014-79-C-0370. The report is entitled: "Bottom Loss Upgrade Final Report", SAI-82-488-WA. The classification of the report is UNCLASSIFIED. One copy of the report is provided for your review and specification of the ultimate distribution list. Copies of the SAI technical reports that document specific results either have been sent previously or are being transmitted under separate cover. If you have any questions concerning the report please contact me at (703) 821-4565.

Also attached is the required DD-250 "Material Inspection and Receiving Report" covering the services provided under the subject contract.

SAI would appreciate execution of Block 21B to indicate your acceptance of items 0001 and A002.

In accordance with Section I under subject contract please forward the signed DD-250 within four (4) days after its receipt to the appropriate payment office. Also, please forward SAI's executed copy to the following address:

Science Applications, Inc.
1710 Goodridge Drive
P.O. Box 1303
McLean, VA 22102
ATTN: Barbara Orndorff
Mail Station 12-2

It has been a pleasure working with you and your office and SAI looks forward to future NORDA projects.

Sincerely,

John S. Hanna
Ocean Acoustics Division

Enclosure

Accession For	<input checked="" type="checkbox"/>	<input type="checkbox"/>	<input type="checkbox"/>
NTIS GRA&I			
DTIC TAB			
Unannounced			
Justification			
By			
Distribution/			
Availability Codes			
Dist and/or			
Special			
			A

BOTTOM LOSS UPGRADE
Final Report

SAI 82-488-WA

May 1981

Prepared by:

E. Michelson
L. Dozier
A. Stokes
R. Greene

Prepared for:

E. D. Chaika
Naval Ocean Research and Development
Activity (NORDA)

Prepared Under Contract No. N00014-79-C-0370

SCIENCE APPLICATIONS, INC.

1710 Goodridge Drive
P.O. Box 1303
McLean, Virginia 22102
(703) 821-4300



UNCLASSIFIED

SECURITY CLASSIFICATION OF THIS PAGE (When Data Entered)

208

REPORT DOCUMENTATION PAGE		READ INSTRUCTIONS BEFORE COMPLETING FORM
1. REPORT NUMBER SAI 82-488-WA	2. GOVT ACCESSION NO. AD-A099478	3. RECIPIENT'S CATALOG NUMBER
4. TITLE (and Subtitle) Bottom Loss Upgrade	5. TYPE OF REPORT & PERIOD COVERED Final Report April 1, 1981 - June 1, 1981	
	6. PERFORMING ORG. REPORT NUMBER SAI 82-488-WA	
7. AUTHOR(s) E. Michelson, L. Dozier, A. Stokes, and R. Greene	8. CONTRACT OR GRANT NUMBER(s) N00014-79-C-0370 New	
	9. PERFORMING ORGANIZATION NAME AND ADDRESS Science Applications, Inc. 1710 Goodridge Dr., P.O. Box 1303 McLean, VA 22102	
11. CONTROLLING OFFICE NAME AND ADDRESS Naval Ocean Research & Development Activity NSTL Station Bay St. Louis, MS 39529	10. PROGRAM ELEMENT, PROJECT, TASK AREA & WORK UNIT NUMBERS	
	12. REPORT DATE May 1981	
14. MONITORING AGENCY NAME & ADDRESS (If different from Controlling Office)	13. NUMBER OF PAGES 24	
	15. SECURITY CLASS. (of this report) UNCLASSIFIED	
	15a. DECLASSIFICATION/DOWNGRADING SCHEDULE	
15. DISTRIBUTION STATEMENT (of this Report) Unlimited		
17. DISTRIBUTION STATEMENT (of the abstract entered in Block 20, if different from Report) Unlimited		
16. SUPPLEMENTARY NOTES		
19. KEY WORDS (Continue on reverse side if necessary and identify by block number) Thin Sediment Bottom Interaction, Bottom Loss, Ocean Acoustics, Thick Sediment Geophysical Model, Acoustic Coherence		
20. ABSTRACT (Continue on reverse side if necessary and identify by block number) A geophysical bottom model for thick sediment bottom-loss is developed using NADC bottom loss data. In addition, NADC thin sediment bottom loss data is used to develop a model for use in ascertaining dominant loss mechanisms of thin sediments. Finally, an investigation to determine the feasibility of using existing random-media propagation models to relate coherence of the acoustic field to spatial variability.		

DISTRIBUTION STATEMENT A
Approved for public release;
Distribution Unlimited

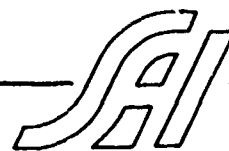
DD FORM 1 JAN 73 1473

EDITION OF 1 NOV 65 IS OBSOLETE
S/N 0162-LF-014-6601

UNCLASSIFIED
SECURITY CLASSIFICATION OF THIS PAGE (When Data Entered)

TABLE OF CONTENTS

	<u>Page</u>
Section 1: INTRODUCTION AND BACKGROUND	1-1
Section 2: GEOPHYSICAL BOTTOM MODEL.	2-1
Section 3: THIN SEDIMENT LOSS MECHANISMS	3-1
3-1 SOUND SCATTERING FROM ROUGH OCEAN BASEMENT.	3-2
3-2 COMPUTER IMPLEMENTATION	3-8
Section 4: THICK SEDIMENT COHERENCE.	4-1
REFERENCES.	R-1



Section 1
INTRODUCTION AND BACKGROUND

The Acoustic Bottom Interaction contract (N00014-79-C-0370) consists of three tasks, which are summarized as follows:

1. Develop a geophysical bottom model using NADC bottom-loss data and other available acoustical and geophysical data, from which low frequency bottom-loss versus grazing angle and frequency can be derived.
2. Examine the NADC thin-sediment bottom-loss data to ascertain the dominant loss mechanisms.
3. Investigate the feasibility of identifying the limits on the likely range of spatial variability of small-scale structure in unconsolidated sediments, and determine the feasibility of using existing random-medium propagation models to relate coherence of the acoustic field to this spatial variability.

Section 2

GEOPHYSICAL BOTTOM MODEL

SAI has developed a geophysical bottom model based on NADC bottom loss data and available geophysical data. The word model is used in two senses. In the first instance, the parameters necessary to specify sediment acoustic properties are identified. Following that, specific models in the form of a numerical data base are evaluated and extrapolated over regions covering the northern hemisphere. The result is called a geophysical model since the acoustical volume properties of the sediment, such as velocity and attenuation profiles, are used and are related to the geological history of the sediment.

A set of ten geophysical parameters are identified that give good agreement between predictions and NADC bottom loss data. This is accomplished using a ray theory model which includes the effects of discontinuities and sound speed and attenuation profiles. For purposes of comparing with data, the known processing artifacts due to Lloyd's mirror and octave processing are also modeled. The ten parameters are: sound speed ratio of the water/sediment interface, two parameters describing the sound speed profile, two parameters for the attenuation profile, bulk sediment density, thin surface reflection with an associated density and thickness, and a sediment thickness and basement reflection coefficient. A brief discussion of each parameter follows.

The sediment sound speed profile is based on Hamilton's (1979) average estimates of profiles for sediments that have terrigenous, calcareous, or silicious content. These profiles are modified somewhat by the fact that sound speed varies at the sediment top, and is governed by a sound speed ratio, i.e., the ratio of sediment-to-water sound speeds at their interface. These ratios are estimated from NADC data. Our estimates of the ratios agree fairly well with estimates based on our best understanding of local geology and Hamilton's (1980) canonical estimates.

The sediment attenuation profile increases linearly with depth. It is the least well understood acoustic property of sediments, but this form of profile is consistently required to fit NADC bottom loss measurements over the full range of geological and physiographic environments.

Sediment density and thin layer density and thickness are an approximation of the actual reflection process in the sediment. In reality, the sediment reflection process cannot be modeled as a two fluid problem. Sediments are generally layered due to different epochs of geological deposition. This is particularly true in abyssal plains. They have many small acoustic reflections near their surface that contribute to the reflected signal, and can produce strong reflections, which are extended in time. When the signal is processed using total energy, multiple layers can be lumped into a single layer to give a good approximation of the reflection process. This is verified independently by workers at ARL in Austin, Texas. Sediment thicknesses are estimated on a world wide basis and presented in the form of contour maps. This data is

interpolated to produce sediment thicknesses in a sixth of a degree data base. These results are based on partial results from Lamont Doherty Geological Observatory and bathymetry information. Basement reflectivity is modeled with a single reflection coefficient, and is sufficient for thick sediment areas.

Geological information is used to support the extrapolation of results of the acoustical measurements at specific sites to the full ocean bottom. This is derived from a variety of sources, predominantly from reports of the Deep Sea Drilling Project (DSDP). Other information of a general nature is available in the standard geological literature in well explored areas such as the Bermuda Rise and the Greenland UK gap. Information relating to the Navy long-range propagation problem is organized by bottom-loss region for the Northern hemisphere south of 70° north. This consists mainly of grain size and chemical composition of bulk and surface sediments for each area as well as physiographic province and history of deposition. Grain size and chemical composition is used to estimate properties of sound speed ratio and depth dependence of the sound speed profile. This together with the history of sediment deposition is used to extrapolate measured acoustic properties to areas where no direct acoustic measurements are available.

The geological analysis has been a very large part of this task since geological information is extensive and scattered throughout the literature. Furthermore, where it is organized it is generally to support a geological hypothesis such as sea floor spreading. In

this case, acoustic information is not highlighted and in some cases is suppressed. It should be emphasized here that while the bulk of geological exploration has dealt with the average properties of deep sediments, Navy acoustic propagation is governed by the detailed properties of near surface sediments. The current project provides the first world wide compilation of geological information relevant to the Navy propagation problem. Together the acoustical measurements and geological information have led to the identification of the relevant acoustic parameters, and their correlation with geological properties of sediments. This has led to the ability to extend our estimates of acoustic parameters to areas where geological information is known. On this basis, a consistent set of geoacoustic model parameters have been assigned for deep ocean areas of the northern hemisphere.

Section 3
THIN SEDIMENT LOSS MECHANISMS

Task 2 is comprised of two sub tasks that examine NADC thin-sediment bottom-loss data in the context of a mathematical/computer model. The model attempts to reconcile the data with known sediment refraction and loss mechanisms and a model for rough basement random scattering. The data are used to initially estimate geophysical and model parameter inputs for the specific ocean region and measurement configuration where the data were obtained. These data characteristically show modest to high bottom-losses at nearly all angles and frequencies, with loss increasing with frequency but nearly independent of grazing angle. Any proposed model must conform to these data characteristics in order to correctly ascertain the dominant loss mechanisms.

The first sub task concerns a rough surface scattering model that would be appropriate for basement scattering and consistent with the data behavior. A detailed description of such a mathematical model follows below. The second sub task concerns the computer implementation of the rough surface basement scattering model integrated with an appropriate water/sediment refraction and loss model. A detailed description of this implementation follows the mathematical model description.

3.1 SOUND SCATTERING FROM A ROUGH OCEAN BASEMENT

To analyze the effect of a rough ocean basement on sound propagation in the ocean, the following model is used.

The basement is described as a random rough surface, with a zero mean Gaussian distribution of heights. Further, for simplicity, the surface is assumed wide sense stationary, i.e., the correlation function W between two points of the surface depends only on the distance between the points; it is also isotropic, i.e., independent of direction. The surface is then characterized by its root-mean-square (rms) height σ , its correlation distance ℓ , and its power spectrum $S(k)$, the Fourier transform of the correlation function, the rms slope, $\gamma \approx \sigma/\ell$, of the surface is then given by $\gamma = \sqrt{-W''(0)}$. The distribution of surface slopes is again Gaussian, with zero mean.

The assumption of a Gaussian surface allows the use of a composite surface theory due to Brown (1980). The surface is decomposed into two (Gaussian) surfaces, one containing large scale features (small wave number), and superimposed on that, the second, describing small scale (ripple) effects.

The purpose of this decomposition is as follows. Scattering from large scale surface features is dominated by "glints", i.e., specular reflection of the incident plane wave from properly oriented facets of the large surface.

Contributions to the average received intensity of this effect is obtained using the tangent plane (Kirchhoff) method, (geometrical optics solution). Small surface features produce a diffuse scattering, and the intensity contribution is obtained as a first order perturbation of the geometrical optics solution. Since both surface features are independent, the total average intensity is the incoherent sum of these two contributions, as shown by Brown (1980).

The division between large and small scale surfaces is in terms of a surface wave number K_D . The large surface has a spectrum $S_L(K)$ defined by

$$S_L(K) = \begin{cases} S(K), & 0 \leq K \leq K_D, \\ 0, & K > K_D \end{cases}$$

while the small scale surface spectrum $S_S(K)$ is given by

$$S_S(K) = \begin{cases} 0, & 0 \leq K < K_D \\ S(K), & K \geq K_D \end{cases}$$

K_D is determined as follows. The rms height σ_S of small surface features is defined by

$$\sigma_S^2 = 2\pi \int_{K_D}^{\infty} k S(k) dk$$

where K_D is chosen so that the Rayleigh number of small surface features is small, i.e., $4k_0^2 \sigma_S^2 \ll 1$, and k_0 is the

wave number of the incident plane wave. This requirement determines K_D . (In practice, we set $4k_0^2 \sigma_s^2 = .13$, and solved for K_D).

Having determined K_D , the rms slope γ_L of large surface features is given by

$$\gamma_L^2 = -W''(0) = 2\tau \int_0^{K_D} k^3 S(k) dk$$

The Gaussian slope distribution of large surface features is given in terms of γ_L^2 .

The mean scattered intensity from large surface features is given by (see Bass, articles 20 and 24)

$$\overline{|u|^2} = \int_{S_0} \frac{|v|^2 q^4}{4R_1^2 R_2^2 q_z^4} w_e \left(\gamma = \frac{-q_x}{q_z} \right) dS$$

the overbar indicates "average", S_0 is the ensonified area of the ocean basement, and if \vec{K}_1, \vec{K}_2 are the incoming and outgoing wave vectors at the basement, then $\vec{q} = \vec{K}_1 - \vec{K}_2$. \vec{K}_1, \vec{K}_2 have norm k_0 , and incident and azimuthal angles θ_0, ϕ_0 , and θ, ϕ , respectively. The azimuthal angles are measured relative to the plane which contains the source and receiver, and is normal to the ocean floor.

$$q^2 = |\vec{K}_1 - \vec{K}_2|^2 = 2k_0^2 \left[1 + \cos\theta \cos\theta_0 - \sin\theta \sin\theta_0 \cos(\phi_0 - \phi_1) \right],$$

$$q_z = (\vec{K}_1 - \vec{K}_2)_z = k_0 (\cos\theta + \cos\theta_0).$$

$\gamma = -q_{\perp}/q_z$ defines the angle of specular reflection from source to receiver, where $q_{\perp} = (q_x, q_y)$. R_1 and R_2 are distances along the ray paths from source and receiver respectively, to the basement. V is the basement reflection coefficient (set equal to one in this preliminary study).

w_e is the effective distribution of surface slopes of large scale surface features in the presence of shadowing. Following Bass (articles 23 and 24), and Sancer (1969)

$$w_e \left(\gamma = \frac{-q_{\perp}}{q_z} \right) = w \left(\gamma = \frac{-q_{\perp}}{q_z} \right) R(\theta, \theta_0),$$

where $w(\gamma_x, \gamma_y)$ is the slope density function of large surface features given by

$$w(\gamma_x, \gamma_y) = \frac{1}{2\pi\gamma_L^2} \exp \left(\frac{-(\gamma_x^2 + \gamma_y^2)}{2\gamma_L^2} \right).$$

$R(\theta, \theta_0)$ is a correction due to shadowing, given by

$$R(\theta, \theta_0) = \left[1 + C(\theta) + C(\theta_0) \right]^{-1},$$

$$\text{with } 2C(\theta') = \left(\frac{2\gamma_L^2}{\pi} \right)^{1/2} \tan\theta' \cdot \exp \left(\frac{-\cot^2\theta'}{2\gamma_L^2} \right),$$

$$- \operatorname{erfc} \left(\frac{\cot\theta'}{(2\gamma_L^2)^{1/2}} \right)$$

(Strictly speaking, the above formula for R is correct if $\phi_0 - \phi$ (the azimuthal difference) is near π . For back scattering, ($\phi_0 - \phi \sim 0$), the term $C(\theta) + C(\theta_0)$ should

be replaced by $C(\max(\theta, \theta_0))$. In the absence of any shadowing theory providing a transition between $\phi_0 - \phi \sim \pi$ and $\phi_0 - \phi = 0$, it was decided to use the above formula for all $\phi_0 - \phi$. The difference is expected to be slight.)

The perturbation term due to diffuse reflection from small surface features is of the form (see Bass, articles 8 and 24, and Brown),

$$\overline{|u|^2} = \int_{S_0} \frac{2k_0^4}{\pi R_1^2 R_2^2} Q(\vec{\alpha}, \vec{\beta}) R(\alpha, \theta_0) \Gamma(q, \gamma_L, S_S) dS$$

where S_0 , R_1 , R_2 , k_0 , and $R(\phi, \phi_0)$ are as before.

$\vec{K}_1 = k_0 \vec{\alpha}$, $\vec{K}_2 = k_0 \vec{\beta}$, and $Q(\vec{\alpha}, \vec{\beta})$ is given by (for $|v| = 1$),

$$Q(\vec{\alpha}, \vec{\beta}) = (1 - \alpha_{\perp} \cdot \beta_{\perp})^2 = [1 - \sin\theta \sin\theta_0 \cos(\phi_0 - \phi)]^2$$

$\Gamma(q, \gamma_L, S_S)$ is a convolution integral involving the small spectrum S_S and the slope density function for large surface features with limits involving the effects of shadowing.

For this preliminary study, $\Gamma(q, \gamma_L, S_S)$ is approximated by $2\pi S_S(|q|)$. (Brown provides a rationale, using results of Stogryn, for including the shadowing function R within the perturbation integral. The physical notion is that diffuse scattering cannot occur if the small scale surface features are shadowed by large scale features. This approximation for Γ may not be adequate if $\gamma_L^2 q_z^2$ becomes too large.

The total average intensity at the receiver is then

$$\overline{|U|^2 + |u|^2} = \int_{S_0} \frac{1}{R_1^2 R_2^2} K(\theta, \theta_0, \phi_0 - \phi, \sigma, \gamma, S, k_0) dS,$$

where the kernel K has been implicitly given above.

The features of this composite surface theory that makes this model appealing are as follows:

First, as shown by Brown, in the absence of large scale features, one recovers the classical solution (see Rice) for scattering from a slightly perturbed planar surface. In the limit, as $\gamma^2 \rightarrow 0$, the integral produces the specular reflection correctly. Numerically, the approximation of the integral over S_0 is accurate, using a 2000 foot mesh size, down to a mean slope of about 8° . Below that, a smaller mesh size over S_0 is needed to accurately evaluate the specular contribution.

Second, the choice of K_D , and therefore γ_L^2 , depends on k_0 . This introduces a frequency dependence in the geometrical optics solution, an effect which has been observed in radar studies of the moon (see Evans and Hagfors). Of course, the usual geometrical optics solution is a high frequency limit, and is necessarily independent of k_0 .

Third, following Lynch and Wagner (1970a, 1970b) the kernel has been checked for energy conservation. This requires that for all $\theta_0, \phi_0, \sigma, \gamma, S, k_0$,

$$\int_0^{\frac{\pi}{2}} \int_0^{2\pi} K(\theta, \theta_0, \phi_0 - \phi, \sigma, \gamma, S, k_0) \sin \theta \, d\phi \, d\theta = \cos^2 \theta_0.$$

A computation has been made, and the result is correct, up to a factor near 1, at most 1.18. While negligible, the kernel has been re-normalized by a factor of $(1.15)^{-1}$.

It should be noted that the above shadowing theory is a single scatter theory only, containing no correction for multiple scatters. The present theory is adequate in this respect except for very rough surfaces (mean slopes above 40°), and incident angles near zero.

3.2 COMPUTER IMPLEMENTATION

The rough basement scattering integral for total average intensity given above is one part of a complete environmental acoustic model implemented on a computer. A complete model requires that the incident intensity at the sediment/basement interface and at the receiver correctly account for spreading loss and refraction in the water column and refraction and attenuation in the sediment. Since source-to-receiver distances are not great, water column attenuation is not significant. Also, the incremental effects of travel time and spreading loss due to the portion of the ray path within the sediment are small enough to be ignored.

Spreading loss and refraction in the water column (to the water/sediment interface) are computed using a ray trace program with the same source/receiver depths and sound speed profile used by NADC and measured during the actual sea tests. Best estimates of sediment properties are obtained from historical records and other analyses, however sediment thickness is estimated from NADC bottom-loss data

(the procedure used is discussed in detail below), and a constant sound-speed gradient is also estimated. The basement scattering kernel has been described in detail above. Integration over the scattering region is approximated by a summation over a grid representing the ensonified/scattering region.

The first step in the simulation is to compute the ensonified/scattering region at the water/sediment interface over a range of grazing angles from zero to 90 degrees. A family of rays are traced from the ocean bottom to source and receiver depths, allowing up to one surface bounce. By reciprocity these would be the same rays from source/receiver depths to the bottom. A table is generated that records for each ray traced: bottom grazing angle, spreading loss, travel time, arrival angles, and horizontal range from source/receiver to the point of bottom contact. A smooth pressure release surface is assumed.

These tables provide the basic input needed for generating the acoustic field incident on the bottom and scattered field to the receiver for as many source-to-receiver distances as required to compute bottom-loss as a function of grazing angle. The total ensonified area is given by a circle, centered at the source projection on the bottom, of radius equal to the horizontal range to zero grazing angle for a single surface reflected ray leaving the source in an upward direction. Similarly, the scattering region to the receiver is computed as a circle centered at the receiver projection on the bottom. For a given source/receiver distance these two circles intersect if the distance is less than the sum of the two circle's radii, their

intersection being the bottom region from which scattered incident energy can reach the receiver. A uniform grid is then set up to encompass this region and all tabulated ray trace values are interpolated to these grid points. This new table now serves as a basis for computing basement scattering for each source/receiver geometry.

Before this is done, however, a sediment is introduced as follows. For the NADC test site used, a water/sediment sound speed ratio and sediment sound speed gradient are estimated. By examining NADC bottom-loss data, one may also deduce a lower grazing angle cut off below which bottom loss rapidly drops off. Assuming rays incident below this cut off angle do not reach the basement and therefore do not reach the receiver, a sediment thickness can be estimated. Again, using NADC bottom-loss data at large grazing angles a frequency dependent loss is estimated using

$$\text{Loss} = \text{BRL} + 2 \alpha \ell f$$

where BRL = basement reflection loss constant

α = attenuation coefficient/unit length/frequency

ℓ = one way sediment ray path length

f = frequency

Since ℓ can be computed and f is known, the data are used to solve for BRL and α , which is then used to calculate sediment loss for each refracting ray.

The equation for total average received intensity, given in Section 3.1 is modified to account for an inhomogeneous ocean by replacing $(1/R_1^2 R_2^2)$ by $(I_1 I_2)$, (which have been tabulated), at the basement, and summing over the appropriate bottom grid using

$$\overline{I_R} = \sum I_1 I_2 K(\theta, \theta_0, \phi_0 - \phi, \sigma, \gamma, S, k_0) \Delta A$$

subject to any angle or travel time constraints that may be appropriate. At each grid point the effects of the four dominant bottom bounce ray paths are computed, i.e., source, bottom bounce, receiver; source, surface, bottom bounce, receiver; etc.

A time history of arrival intensities is also computed using the specular path travel time (which is minimum bottom bounce path travel time) as reference and a specified time increment bin. Hence, rays arriving within each time increment are subsumed and tabulated along with such other useful related information as average grazing angle, average azimuth angle, number of rays arriving within the interval, etc. These data may also be computer plotted, if desired, to present visual synopses, which are useful for understanding and relating scattering phenomena to the various geophysical mechanisms, e.g., roughness parameters, sediment parameters, etc. This type of output allows a quasi-quantitative comparison with available time history data.

A limited amount of data have been used for program check out, and several rough surface spectra have been tried for the purpose of determining qualitative agreement with data and the degree of surface roughness and sediment properties required.

Work is continuing in this area under a follow-on contract entitled "Thin Sediment Bottom Interaction Measurements". The objective of this contract is to apply the computer code with appropriate bottom acoustic properties and scattering kernel to interpret a set of acoustical data.

Section 4
THICK SEDIMENT COHERENCE

Two issues, which have been identified as having high priority to the Bottom Interaction Programs, (Hanna and Hawker), (Martin), are the rate of lateral variation of sediment properties, in different oceanic regions and the degree of coherence of bottom-interacting energy that propagates through such sediments and is scattered by sediment inhomogeneities. Of fundamental interest is whether this bottom-interacting energy is useful for signal processing systems.

The final report for this task (Dozier, 1981) (cf. Enclosure) shows the feasibility of using an extension of an existing random-medium propagation model (Dozier and Tappert, 1978) to relate coherence of the acoustic field to lateral variability of sediments. The approach is a coupled-mode theory valid in a low-frequency limit; of course, low frequencies are precisely where acoustic interaction with sediment is important. A significant complication not included in the earlier work, (ibid.) however, is the inclusion of a sediment model, with density and attenuation as well as sound speed. Rutherford and Hawker (1978) have shown that sediment density gradients play a very minor role in bottom reflection loss; hence, we choose a layered sediment model in which density is constant within each layer. Sediment sound speed is then modeled as varying randomly about a mean, deterministic profile in depth. Although in fact, unlike the earlier case of internal waves in the water column (Dozier, JASA 63, 1978), the sediment sound speed is deterministic, we lack detailed subbottom

data and, even if it were available, it would be too complex to be useful. For our purposes the scale length of horizontal variation is the important feature, and is the key ingredient of our random model.

Thus, we derive a random coupled mode equation which describes statistically the coupling between the deterministic normal modes of our mean sound speed profile, given attenuation and piecewise constant density. (Lateral variations in density and attenuation can be included also, but are relatively unimportant and unnecessarily complicate the coupled mode equation.) Unlike the previous reference however, the coupling coefficients are now complex (because of attenuation), and are neither symmetric nor hermitian. The coupled mode equation, therefore, loses its energy-conserving property as expected, due to attenuation.

The next step is averaging the coupled mode equations to obtain a master equation for the mean acoustic intensity. Although non-conservation is a significant complication, averaging can still be done. The master equation's coefficient matrix is no longer symmetric, and modal energies do not approach equipartition.

Next, the averaging is extended to include a two-point statistic of horizontal coherence transverse to the direction of propagation and for separation distances much less than the source range. This is done in a quasi-static manner by treating horizontal distance as a parameter, just as time was treated earlier, (Tappert and Dozier, 1978), and results in a master equation for horizontal coherence.

A question now is, when is the averaging mathematically valid? It is done using a perturbation technique, but without precise knowledge of the horizontal distance parameter or of the domain of validity. The distance parameter is essentially determined by the product of rms sound speed variation and correlation length of the variation (Dozier, JASA 63, 1978). Typical rms variations found by Matthews (1980) are 10% (relative to the mean) for calcareous sediments and 20% for turbidite sediments. Houtz (1980) finds (experimentally) standard deviations mostly from 10% to 15% over large areas of the North Atlantic. These relative variations are roughly 10 times the relative variation of sound speed due to internal waves. On the other hand, Tyce, et. al., (1980), have found high lateral variability, suggesting that the correlation length of the random sound speed function is much less than the 11 km distance for internal waves in Dozier (1981). Since, as noted above, it is the product of correlation length and rms sound speed variation that essentially determines the perturbation parameter, we expect a domain of validity comparable to that found for internal waves, i. e., up to perhaps 400 Hz. This includes most of the low-frequency regime where bottom interactions are important.

Until more bottom data becomes available, the primary value of this model is to bound the coherence problem. For lateral variability within the model's estimated domain of validity, a numerical implementation will yield the associated loss of coherence. Comparing model results for different scales of lateral variability will illustrate trends (e.g., loss of coherence with increasing

rms sound speed variation, with correlation length held fixed; and vice versa) and point out worst cases. Certainly, for many real ocean environments the model should predict whether a significant loss of coherence is likely.

Unfortunately, numerical implementation of this model was beyond the scope of this contract, but we hope to be able to do this in future BIP work.

REFERENCES

- Bass, F. G. and I. M. Fuks, Wave Scattering from Statistically Rough Surfaces, Pergamon Press, N.Y., 1979.
- Brown, G. S., "Backscattering from Gaussian - Distributed Perfectly Conducting Rough Surfaces," IEEE TR AP, AP-26, 472-482, 1978.
- _____, Corrections to "Backscattering from a Gaussian - Distributed Perfectly Conducting Rough Surface," IEEE TR. AP, AP-28, 943-946, 1980.
- Dozier, L. B., "A Coupled-Mode Model for Spatial Coherence of Bottom-Interacting Energy," Report SAI-82-4769-WA, Science Applications, Inc., May, 1981.
- _____, and F. D. Tappert, "Statistics of normal mode amplitudes in a random ocean. I. Theory," J. Acoust. Soc. Am. 63, 353-365, 1978.
- _____, "Statistics of normal mode amplitudes in a random ocean. II. Computations," J. Acoust. Soc. Am. 64, 533-547 (1978).
- Evans, J. V. and T. Hagfors, Radar Astronomy, Chap.5, McGraw-Hill, N.Y., 1968.
- Hamilton, E. L., "Sound Velocity Gradients in Marine Sediments," P. 909-922, J. Acoust. Soc. Am. 65(4), April 1979.
- _____, "Geoacoustic Modeling of the Sea Floor," p. 1313, 1340, J. Acoust. Soc. Am. 68(5), Nov. 1980.
- Hanna, J. S., and K. E. Hawker, "Identification of the Exploratory Development Bottom Interaction Issues for Passive Detection Application (U)," NORDA Report, Feb. 1979 (SECRET).
- Houtz, R. E., "Comparison of Velocity-Depth Characteristics in Western North Atlantic and Norwegian Sea sediments," J. Acoust. Soc. Am. 68, 1409-1414 (1980).

REFERENCES (CONTINUED)

Lynch, P. J., and R. J. Wagner, "Energy Conservation for Rough-Surface Scattering," J. Acoust. Soc. Am. 47, 816-821, 1979a.

_____, and R. J. Wagner, "Rough-Surface Scattering: Shadowing, Multiple Scatter, and Energy Conservation," J. of Math. Phys. 11, 3032-3042, 1970b.

Martin, R. L., Chairman, "Coordinated Program Plan for Acoustic Bottom Interaction (U)", prepared by the Bottom Interaction Panel of the ASW Coordinating Panel on Ocean Acoustics (R. L. Martin, Chairman), Environmental Requirements and Program Analysis Office, NORDA, 7 March 1980 (CONFIDENTIAL).

Matthews, J. E., "Heuristic physical property model for marine sediments," J. Acoust. Soc. Am. 68, 1361-1370, 1980.

Rice, S. O., "Reflection of electromagnetic waves from a slightly rough surface," Comm. Pure and Appl. Math 4, 351-378, 1951.

Rutherford, S. R., and K. E. Hawker, "Effects of density gradients on bottom reflection loss for a class of marine sediments," J. Acoust. Soc. Am. 63, 750-757, 1978.

Sancer, S. I., "Shadow corrected electromagnetic scattering from a randomly rough surface," IEEE TR. AP, AP-17, 577-585, 1969.

Stogryn, A., "Electromagnetic scattering from rough, finitely conducting surfaces," Radio. Sci., 2, 415-428, 1967.

Tappert, F. D., and L. B. Dozier, "Acoustic power spectra due to multiple internal wave scattering," J. Acoust. Soc. Am. 63, S23 (1978).

Tyce, R. C., L. A. Mayer, and F. N. Spiess, "Near-bottom seismic profiling: High lateral variability, anomalous amplitudes, and estimates of attenuation," J. Acoust. Soc. Am. 68, 1391-1402 (1980).